Toward a consistent model for strain accrual and release for the New Madrid Seismic Zone, central United States

Susan E. Hough[1] and Morgan Page[1]

Received 14 June 2010; revised 1 December 2010; accepted 3 January 2011; published 25 March 2011.

[1] At the heart of the conundrum of seismogenesis in the New Madrid Seismic Zone is the apparently substantial discrepancy between low strain rate and high recent seismic moment release. In this study we revisit the magnitudes of the four principal 1811–1812 earthquakes using intensity values determined from individual assessments from four experts. Using these values and the grid search method of Bakun and Wentworth (1997), we estimate magnitudes around 7.0 for all four events, values that are significantly lower than previously published magnitude estimates based on macroseismic intensities. We further show that the strain rate predicted from postglacial rebound is sufficient to produce a sequence with the moment release of one M_{max}6.8 every 500 years, a rate that is much lower than previous estimates of late Holocene moment release. However, M_w6.8 is at the low end of the uncertainty range inferred from analysis of intensities for the largest 1811–1812 event. We show that M_w6.8 is also a reasonable value for the largest main shock given a plausible rupture scenario. One can also construct a range of consistent models that permit a somewhat higher M_{max}, with a longer average recurrence rate. It is thus possible to reconcile predicted strain and seismic moment release rates with alternative models: one in which 1811–1812 sequences occur every 500 years, with the largest events being M_{max}~6.8, or one in which sequences occur, on average, less frequently, with M_{max} of ~7.0. Both models predict that the late Holocene rate of activity will continue for the next few to 10 thousand years.

Citation: Hough, S. E., and M. Page (2011), Toward a consistent model for strain accrual and release for the New Madrid Seismic Zone, central United States, *J. Geophys. Res.*, *116*, B03311, doi:10.1029/2010JB007783.

1. Introduction

[2] The New Madrid Seismic Zone (NMSZ) has produced three well-documented sequences: the historic sequence in 1811–1812 [e.g., *Fuller*, 1912; *Johnston and Schweig*, 1996], and apparently similar sequences around 900 A.D. and 1450 A.D. [*Tuttle et al.*, 2002]. There is additionally more limited geological evidence for large events around 300 A.D. and 2350 B.C. [*Tuttle et al.*, 2005].

[3] The 1811–1812 New Madrid earthquake sequence included three well-documented main shocks that have been described and analyzed in considerable detail, plus a large aftershock that is considered the fourth principal event in the sequence [e.g., *Mitchill*, 1815; *Fuller*, 1912; *Nuttli*, 1973; *Penick*, 1981; *Street*, 1982, 1984; *Johnston*, 1996b; *Hough et al.*, 2000; *Bakun and Hopper*, 2004]. The three principal main shocks occurred at approximately 0215 LT on 16 December 1811; around 0915 LT on 23 January 1812, and approximately 0345 LT on 7 February 1812 (hereafter referred to as NM1, NM2, and NM3, respectively). The so-called dawn aftershock, on 16 December 1811, occurred at 0715 LT on 16 December 1811 (hereafter referred to as NM1A). Published magnitude estimates of the four principal events range from ~7 to over 8 [e.g., *Nuttli*, 1973; *Johnston*, 1996b; *Newman et al.*, 1999; *Hough et al.*, 2000; *Bakun and Hopper*, 2004].

[4] The tectonic strain rate in the NMSZ has been investigated in a series of studies based on GPS observations. As the GPS data have provided increasing resolution, the bounds on the maximum possible strain rate have decreased [e.g., *Calais et al.*, 2006; *Calais and Stein*, 2009]. Although higher values have been inferred by earlier studies [e.g., *Liu et al.*, 1992; *Gan and Prescott*, 2001], the most recent and reliable analysis reveals root-mean-square velocities of less than 0.2 mm/yr in the NMSZ. If this were a two-dimensional rate distributed over a zone 150 km wide, it would correspond to a strain rate bound of 1.3×10^{-9}/yr. Reconsidering GPS observations over a 10 year period, *Boyd et al.* [2010] do find a small but resolvable nonzero slip rate, on the order of 0.3 mm/yr, at a station near New Madrid. They show that the GPS observations can be explained by a finite dislocation beneath the Reelfoot fault slipping at 1.5 mm/yr. As illustrated by the results of *Kenner and Segall* [2000], present-day surface deformation rates provide at best a very weak constraint on strain rate if one appeals to a model that involves localized stress on finite, buried fault.

[1]U.S. Geological Survey, Pasadena, California, USA.

[5] A number of studies consider the predicted strain rate associated with postglacial rebound in central/eastern North America [e.g., *Wu and Johnston*, 2000; *Grollimund and Zoback*, 2001; *Mazzotti et al.*, 2005]. *Grollimund and Zoback* [2001] show that postglacial rebound coupled with a locally weak crust predicts a strain rate in the NMSZ on the order of 10^{-9}/yr over a region of 20,000–40,000 km^2. Along the St. Lawrence River valley in Quebec, the strain rate associated with postglacial rebound is higher, generating a vertical uplift of 2.6 ± 0.4 mm/yr [*Mazzotti et al.*, 2005]. This signal is resolvable with available GPS data, and is consistent, within the uncertainties associated with a short historical catalog, with the historic rate of large earthquakes [*Mazzotti et al.*, 2005]. In general, comparisons of geodetic and seismic strain rates in low strain rate regions are hampered by the short historic record and significant uncertainties in magnitudes of large historical earthquakes [e.g., *Ambraseys*, 2006]. In this report we revisit the magnitudes of the principal 1811–1812 earthquakes using newly developed average intensity values, and reconsider the long-term distribution of magnitudes for the NMSZ. We then compare our results with the moment release rate predicted from postglacial rebound in the NMSZ.

2. Intensities of the 1811–1812 Main Shocks

[6] We revisit the magnitude estimates for the principal 1811–1812 main shocks. Magnitudes for these events have been estimated a number of different ways, including from strain rate considerations [e.g., *Newman et al.*, 1999; *Calais et al.*, 2006], and the extent and scale of liquefaction features [e.g., *Obermeier*, 1996]. However, analysis of macroseismic data provides the most direct available constraint on magnitude. The method initially presented by *Bakun and Wentworth* [1997] has been widely used in recent years to analyze intensity values of historical earthquakes. This method, which uses a grid search approach and an intensity-attenuation relation determined from instrumentally recorded calibration events, is attractive because it obviates the need for subjectively drawn isoseismals, and it yields an objectively determined optimal magnitude and location. Two primary sources of uncertainty remain, however: that associated with the regional attenuation relation, and that associated with the intensity values.

[7] If one relies solely on regional calibration events, one typically faces the limitation of having only calibration events that are smaller than the largest historical earthquakes. To obviate this limitation, *Johnston* [1996a] analyzes calibration events from geologically analogous settings, other stable continental regions (SCR) worldwide. A number of recent studies, however, have found that intensity attenuation is not comparable across different SCR regions [e.g., *Bakun and McGarr*, 2002; *Szeliga et al.*, 2010]. *Bakun et al.* [2003], and later *Bakun and Hopper* [2004], use only events from central/eastern North America to develop their attenuation relations. Their set of calibration events includes only a single $M_w > 7$ earthquake, the 1929 Grand Banks, Newfoundland, earthquake. This event occurred well offshore and is arguably not a true SCR event because the propagation of *Lg* waves across the relatively complex continental margin is likely to be less efficient than propagation through more uniform SCR crust. Accordingly, one arrives back at the need to extrapolate attenuations beyond the magnitude range for which they are constrained. The degree of variability associated with this extrapolation is illustrated by the difference between magnitude estimates determined using the different attenuation models presented by *Bakun et al.* [2003] and *Bakun and Hopper* [2004]. The two models, hereinafter models 1 and 3 (following *Bakun and Hopper* [2004]), differ only in the mathematical approach to extrapolation. In this study we report magnitude estimates using both attenuation models. We focus on this method because in recent years, the results of *Bakun and Hopper* [2004] have been taken by many to support the 1811–1812 main shock magnitude values given highest weight in the calculation of the national seismic hazard maps [*Petersen et al.*, 2008].

[8] The uncertainties and variability associated with intensity assignments are rarely considered. In many studies, published intensity values are used as input data, uncritically. Intensity values are not, however, data, but rather interpretations. Any number of studies have discussed the issues that must be considered carefully in the interpretation of macroseismic data [e.g., *Ambraseys*, 1983; *Ambraseys and Bilham*, 2003] The initial interpretation of intensities for the principal New Madrid earthquakes is presented by *Nuttli* [1973] and was expanded by *Street* [1982, 1984]. *Hough et al.* [2000] revisit the archival accounts of the earthquakes and conclude that many of the initial intensity assignments were too high, including a few outright transcription errors and a greater number of values that are higher than would be assigned given present-day understanding of macroseismic effects. For example, although the principal 1811–1812 events caused dramatic secondary effects in the Mississippi River Valley, recent studies [e.g., *Ambraseys and Bilham*, 2003] show that such effects are not reliable indicators of overall shaking intensity. Further, while according to traditional intensity scales, MMI IV–V shaking is required to awaken many or most sleepers, reliably determined "Did You Feel It"? [*Wald et al.*, 1999] intensities reveal that during large regional earthquakes, sleepers are generally awakened by MMI III–IV shaking.

[9] Although the intensity values determined by *Hough et al.* [2000] are justified in detail, they are themselves subjective. In an effort to explore the consequences of subjective individual intensity assignments, in this study we develop a set of intensity values for the four principal New Madrid earthquakes on the basis of independent assessments by multiple experts (Tables 1–4). A similar approach was employed by *Bollinger* [1977] to determine intensity values for the 1986 Charleston, South Carolina, earthquake. For shorthand we refer to the results as consensus intensity values, although we note that they represent an average of independent assessments rather than true consensus values.

[10] To explore the variability associated with individual intensity assignments and to develop a set of consensus intensities, intensity values were assigned independently by four researchers with experience in historical earthquake research. The assignments were done using all accounts available at this time. Although additional accounts have reportedly been collected (A. Johnston, personal communication, 2009), they have not been made available to the community. Most of the accounts are from the compilation of *Street* [1982, 1984], supplemented by a small number of additional sources. Additionally, photographs are included

Table 1. Intensity Assignments for 0215 LT, 16 December 1811, Main Shock

Location	Longitude (deg)	Latitude (deg)	MMI1	MMI2	MMI3	MMI4
Abingdon, Va.	−81.981	36.708	NF	NF	NF	NF
Alexandria, Va.	−77.044	38.812	4.5	5.0	4.5	5.0
Allegany, N. Y.	−78.494	42.090	3.1	4.5	4.5	4.0
Asheville, N. C.	−82.564	35.593	4.5	5.5	5.0	5.0
Augusta, Ga.	−81.994	33.470	5.0	5.0	4.5	5.0
Baltimore, Md.	−76.626	39.287	F	F	F	F
Birdsville, Ky.	−88.450	37.220	7.0	5.5	7.0	NA
Brownsville, Pa.	−79.889	40.020	F	3.0	2.0	3.0
Carthage, Tenn.	−85.955	36.263	6.5	6.5	7.5	5.0
Charleston, S. C.	−79.940	32.798	5.5	4.5	4.5	5.0
Charleston, N. H.	−72.423	43.238	F	F	F	NA
Chillicothe, Ohio	−82.985	39.330	4.5	4.0	5.5	5.0
Cincinnati, Ohio	−84.517	39.103	6.5	5.5	6.0	5.0
Circleville, Ohio	−82.949	39.594	4.0	5.0	4.5	NA
Clarksburg, Ohio	−83.153	39.506	4.0	3.0	3.0	5.0
Clinton Hill, Ill.	−89.989	38.551	4.0	4.0	4.5	6.0
Columbia, Tenn.	−87.035	35.617	4.0	4.0	4.5	5.0
Columbia, S. C.	−81.040	34.000	6.0	4.5	5.5	5.0
Coosawatchie, S. C.	−80.939	32.588	4.0	4.0	5.0	6.0
Dayton, Ohio	−84.188	39.739	5.0	5.0	5.0	5.0
Dorena, Mo.	−89.240	36.617	7.5	6.0	8.0	8.0
Dover, Tenn.	−87.842	36.488	F	F	NA	NA
Edenton, N. C.	−76.602	36.066	5.0	4.0	5.5	4.0
Fort Massac, Ill.	−88.687	37.143	7.0	6.0	7.5	7.0
Fort Osage, Mo.	−92.032	38.553	6.5	4.5	6.5	6.0
Frankfort, Ky.	−84.881	38.205	6.5	4.5	6.5	6.0
Ft. Dearborne	−83.244	42.305	F	F	F	5.0
Ft. Pickering	−90.000	35.830	F	5.0	7.0	6.0
Ft. Stoddart, Ala.	−88.050	31.270	F	F	F	NA
Ft. Wayne, Ind.	−85.150	41.051	F	F	F	NA
Ft. Stephens	−87.980	31.600	4.0	4.0	4.5	6.0
Georgetown, S. C.	−79.308	33.382	5.0	4.0	5.0	6.0
Goose Creek, S. C.	−80.047	33.000	4.0	<6.0	4.0	NA
Goshen, Ill.	−90.000	38.739	4.0	3.0	5.0	5.0
Henderson City	−87.594	37.837	6.0	6.0	6.5	7.0
Herculaneum, Mo.	−90.379	38.226	4.5	5.5	5.0	6.0
Hodgenville, Ky.	−85.750	37.57	NA	3.5	3.5	5.0
Hopkins City	−87.700	37.350	F	F	6.0	5.0
Hudson, N. Y.	−73.794	42.255	F	F	F	3.0
Jeffersonville	−85.730	38.310	NA	3.0	3.0	5.0
Knoxville, Tenn.	−83.920	35.978	4.5	5.0	4.5	4.0
Lancaster, Ohio	−82.599	39.714	4.0	3.5	4.0	5.0
Laurens, S. C.	−82.020	34.504	6.0	5.0	6.0	5.0
Lebanon, Ohio	−84.210	39.430	NA	4.5	4.5	5.0
Lexington, Ky.	−84.508	38.041	4.5	4.0	4.0	5.0
Louisville, Ky.	−85.777	38.251	4.0	6.5	5.0	5.0
Marietta, Ohio	−81.455	39.417	4.5	4.0	5.0	5.0
Maysville, Ky.	−83.744	38.636	4.5	5.0	F	NA
Meadsville, Pa.	−80.144	41.647	4.0	4.0	5.0	5.0
Milledgeville	−83.237	33.087	5.0	4.0	4.5	4.0
Muhlenberg City	−87.150	37.220	5.0	5.5	NA	5.0
Nashville, Tenn.	−86.784	36.166	5.5	6.0	6.5	7.0
Natchez, Miss.	−91.402	31.562	5.0	5.0	F	6.0
Natchitoches, La.	−93.101	31.760	4.5	5.0	6.0	6.0
New Bourbon, Mo.	−90.021	37.950	6.0	6.5	8.0	8.0
New Haven, Conn.	−72.930	41.304	2.5	F	F	3.0
New Orleans, La.	−90.069	29.971	NF	NF	NF	NF
New York, N. Y.	−73.996	40.728	NF	NF	NF	NF
Newberry, S. C.	−81.614	34.283	6.0	5.5	6.5	NA
Newport, Ky.	−84.496	39.090	6.5	5.5	7.0	6.0
Norfolk, Va.	−76.277	36.849	5.0	5.0	5.0	4.0
Norwich, N. Y.	−75.490	42.510	NA	3.5	3.5	3.0
Ozark Vill., Ark.	−92.200	38.500	F	6.0	7.5	7.0
Pineville, S. C.	−80.029	33.428	F	5.0	6.0	6.0
Pittsburgh, Pa.	−79.983	40.440	4.5	5.0	4.5	5.0
Raleigh, N. C.	−78.647	35.791	3.5	4.0	3.5	3.0
Red Banks, Ky.	−87.593	37.838	7.0	6.5	7.5	7.0
Richmond, Va.	−77.480	37.530	F	3.0	4.0	4.0
St. Louis, Mo.	−90.217	38.631	7.0	6.0	7.0	6.0
Salem, N. C.	−80.260	35.102	4.0	4.5	3.5	4.0
Savannah, Ga.	−81.091	32.064	3.5	3.5	4.5	3.5
Sevierville, Tenn.	−83.574	35.865	3.0	4.0	4.0	4.0

Table 1. (continued)

Location	Longitude (deg)	Latitude (deg)	MMI1	MMI2	MMI3	MMI4
South Union, Ky.	−86.657	36.876	4.0	F	3.5	5.0
Springfield Ohio	−83.844	39.931	5.0	4.0	5.0	5.0
Springfield Tenn.	−86.868	36.524	5.0	3.5	3.5	5.0
Stokes City, N. C.	−80.400	36.300	NA	F	F	4.0
Strasburg, W. Va.	−78.365	38.994	5.0	5.0	5.0	4.0
Vincennes, Ind.	−87.525	38.679	F	6.5	6.5	6.0
Washington, D.C.	−77.026	38.891	4.5	F	4.0	3.0
Washington, Ky.	−83.812	38.611	4.5	4.0	F	5.0
Washington, Miss.	−91.300	31.580	NA	4.0	4.0	5.0
Wheeling, W. Va.	−80.721	40.064	NA	5.0	4.0	5.0
Wilmington, Del.	−75.547	39.746	3.0	F	2.5	2.0
Worthington, Ohio	−83.018	40.093	NA	3.0	3.0	3.0
York, Ontario, Canada	−79.630	43.68	3.0	F	F	NA
Zanesville, Ohio	−82.013	39.940	4.5	4.0	5.0	5.0

to provide an indication of typical historical structures from the era, including a number of buildings that predate the 1811–1812 sequence.

[11] It was left to the discretion of the individual researchers whether an individual account includes sufficient information to infer an intensity value. This determination is

Table 2. Intensity Assignments for Dawn Aftershock of 0715 LT, 16 December 1811

Location	Longitude (deg)	Latitude (deg)	MMI1	MMI2	MMI3	MMI4
Alexandria, Va.	−77.044	38.812	NA	4.5	4.5	3.0
Arkport, N. Y.	−77.697	42.395	4.5	2.5	9.9	3.0
Asheville, N. C.	−82.564	35.593	5.5	5.0	6.5	7.0
Augusta, Ga.	−81.994	33.470	F	F	F	NA
Baltimore, Md.	−76.626	39.287	NA	NA	F	3.0
Brownsville, Pa.	−79.889	40.020	NA	2.0	F	9.9
Carthage, Tenn.	−85.955	36.263	NA	6.0+	F	5.0
Charleston, S. C.	−79.940	32.798	F	5.0	F	NA
Chillicothe, Ohio	−82.985	39.330	F	5.0	4.0	5.0
Cincinnati, Ohio	−84.517	39.103	F	5.5	F	5.0
Circleville, Ohio	−82.949	39.594	4.0	4.5	4.5	NA
Columbia, S. C.	−81.040	34.000	3.0	3.0	4.0+	NA
Ft. St. Stephens	−87.98	31.60	NA	4.5	F	NA
Frankfort, Ky.	−84.873	38.201	NA	5+	F	5.0
Goshen, Ill.	−90.000	38.739	NA	5.0	4.5	3.0
Henderson, Tenn.	−87.594	37.837	4.0	7.5	7.0	7.0
Herculaneum, Mo.	−90.379	38.226	6.0	7.5	6.0	7.0
Hodgenville, Ky.	−85.740	37.574	F	5.1	F	NA
Lancaster, Ohio	−82.609	XXX	F	3.5	4.0	4.0
Lexington, Ky.	−84.508	38.041	F	F	3.0	4.0
Little Prairie, Mo.	−89.60	36.50	10.0	NA	NA	7.0
Louisville, Ky.	−85.777	38.251	NA	7.0	7.0	4.0
Marietta, Ohio	−81.455	39.417	NA	F	4.5	NA
Meadville, Pa.	−80.144	41.647	F	4.5	4.0	4.0
Natchez, Miss.	−91.402	31.562	4.0	F	3.0	NA
Natchitoches, La.	−93.101	31.760	F	F	3.5	NA
New Bourbon, Mo.	−91.525	31.488	5.0	7.5	7.0	6.0
New Madrid, Mo.	−89.40	36.80	NA	7.0	NA	9.0
Newark, N. J.	−74.172	40.736	1.0	1.0	NA	NA
Norfolk, Va.	−76.277	36.849	4.0	5.0	4.5	4.0
Onondaga, N. Y.	−76.141	42.975	F	NA	NA	4.0
Philadelphia, Pa.	−75.164	39.952	3.0	F	2.0	2.0
Pittsburgh, Pa.	−79.983	40.440	4.0	3.5	3.0	4.0
Raleigh, N. C.	−78.647	35.791	3.0	4.5	4.0	3.0
Red Banks, Ky.	−87.593	37.838	4.0	7.5	7.0	7.0
Richmond, Va.	−84.310	37.746	F	F	2.0	3.0
Saint Louis, Mo.	−90.217	38.631	NA	4.5	4.0	6.0
Salem, N. C.	−80.260	36.102	F	F	3.0	3.0
Savannah, Ga.	−81.091	32.064	F	4.5	4.0	3.0
South Union, Ky.	−86.657	36.876	F	4.5	4.0	5.0
Springfield, Tenn.	−86.868	36.524	F	5.0	5.5	5.0
Vincennes, Ind.	−87.525	38.679	NA	6.5	F	NA
Wheeling, W. Va.	−80.721	40.064	4.0	3.5	NA	4.0
Wilmington, Del.	−75.547	39.746	F	2.5	NA	3.0
Worcester, Mass.	−71.802	42.262	1.0	1.0	NA	NA
Zanesville, Ohio	−82.013	39.94	3.0	5.0	NA	5.0

Table 3. Intensity Assignments for 0900 LT, 23 January 1812, Main Shock

Location	Longitude, deg	Latitude, deg	MMI1	MMI2	MMI3	MMI4
Alexandria, Va.	−77.044	38.812	3.5	3.5	4.5	4.0
Annapolis, Md.	−76.492	38.978	4.5	3.5	3.0	3.0
Augusta, Ga.	−81.994	33.470	4.0	4.5	4.0	4.0
Cape Girardeau, Mo.	−89.518	37.306	6.0	9.9	9.9	7.0
Carthage, Tenn.	−85.955	36.263	6.0	6.5	4.5	5.0
Charleston, S. C.	−79.940	32.798	5.5	5.0	4.5	5.0
Chillicothe, Ohio	−82.985	39.330	3.5	4.5	6.5	4.0
Cincinnati, Ohio	−84.517	39.103	4.5	6.0	4.0	5.0
Columbia, S. C.	−81.040	34.000	6.0	6.0	4.0	NA
Coshockton, Ohio	−81.86	40.272	6.0	6.5	6.0	6.0
Dandridge, Tenn.	−83.415	36.015	4.0	4.5	4.5	4.0
Dayton, Ohio	−84.188	39.739	4.5	5.9	5.0	5.0
Detroit, MI	−83.046	42.331	4.5	4.0	NA	4.0
Easton, Md.	−76.076	38.774	4.0	4.0	NA	3.0
Edenton, N. C.	−76.602	36.066	3.5	4.0	4.0	3.0
Ft. Wayne, Ind.	−85.150	41.051	F	F	F	4.0
Frankfort, Ky.	−84.873	38.201	4.0	4.5	4.5	6.0
Georgetown, Ky.	−84.559	38.21	F	F	4.5	5.0
Hartford, Conn.	−72.685	41.764	F	F	4.0	5.0
Hodgenville, Ky.	−85.740	37.574	3.5	5+	4.0	6.0
Jamaica, N. Y.	−73.806	40.691	3.5	4.0	3.0	3.0
Knoxville, Tenn.	−83.920	35.978	3.5	4.5	NA	4.0
Lexington, Ky.	−84.508	38.041	4.0	3.5	4.0	5.0
Louisville, Ky.	−85.777	38.251	6.0	6.5	6.5	6.0
Lower Canada	−79.42	43.77	3.0	F	NA	NA
Marietta, Ohio	−81.455	39.417	3.0	4.0	4.0	4.0
Maysville, Ohio	−83.744	38.636	F	F	F	NA
New Haven, Conn.	−72.930	41.304	4.0	2.0	2.0	3.0
New Orleans, La.	−90.069	29.971	4.0	4.5	4.5	4.0
New York, N. Y.	−73.996	40.728	4.0	F	4.0	3.0
Newark, N. J.	−74.172	40.736	3.0	4.0	3.0	3.0
Newport, Ky.	−84.496	39.090	5.0	6.0	5.5	5.0
Norfolk, Va.	−76.277	36.849	5.0	5.0	5.5	4.0
Nottingham, Md.	−76.490	39.386	4.0	3.0	4.0	2.0
Paris, Ky.	−84.253	38.210	5.0	5.0	4.5	5.0
Raleigh, N. C.	−78.647	35.791	2.5	3.0	3.0	3.0
Richmond, Va.	−77.480	37.530	4.5	5.0	5.5	4.0
Rogersville, Tenn.	−83.016	36.402	4.0	4.0	4.0	NA
Russellville, Ky.	−86.892	36.845	F	F	4.0	NA
Salem, N. C.	−80.260	36.102	F	F	F	4.0
Savannah, Ga.	−81.091	32.064	3.5	4.5	4.5	4.0
Sevierville, Tenn.	−83.574	35.865	4.0	4.0	4.0	5.0
Suffolk, Va.	−76.584	36.726	4.0	5.0	4.5	4.0
Vincennes, Ind.	−87.525	38.679	6.0	6.5	6.5	6.0
Washington, D.C.	−77.026	38.891	3.5	4.0	4.5	4.0
Washington, Ky.	−83.812	38.611	3.0	F	4.0	5.0
Wheeling, W. Va.	−80.721	40.064	4.5	3.5	4.0	4.0
William Henry, N. Y.	−73.710	43.321	F	F	4.0	NA
Worthington, Ohio	−83.018	40.093	3.5	3.0	4.5	5.0
Zanesville, Ohio	−82.013	39.94	4.0	5.0	4.5	4.0

itself subjective. The individual researchers were in agreement that dramatic near-field accounts did not provide the basis for reliable intensity determination. For some of the other accounts, individual researchers reached different conclusions. For NM1 and NM3, which occurred at night, an assignment of "felt" is interpreted as MMI 3.5; for NM1A and NM2, which occurred when many or most people would have been awake, a "felt" is interpreted as MMI 3. Consensus intensities were determined for those accounts for which there were at least three individual intensity values. The number of consensus intensities for each of the principal events is therefore lower than the number of accounts of each earthquake: a total of 86 for NM1 and 45–50 for NM2, NM3, and the dawn aftershock. The values are shown in Figure 1 and listed in Tables 1–4.

[12] The individual intensity assignments for NM1 are shown in Figure 2. The individual assignments reveal no glaring systematic differences, but individual intensity values for a given location do vary considerably, spanning a range of at least 1 full MMI unit for most of the accounts (Figure 3). A similar degree of variability is found for the other three events.

3. Analysis of Consensus Intensities

[13] To analyze the intensity values we use the method of *Bakun and Wentworth* [1997], using both of the published intensity attenuation relations for the central and eastern United States (CEUS). Following *Bakun et al.* [2003] and *Bakun and Hopper* [2004], respectively, we refer to these as models 1 and 3. Our analysis of the consensus intensities

Table 4. MMI Assignments for 0245 LT, 7 February 1812, Main Shock

Location	Longitude (deg)	Latitude (deg)	MMI1	MMI2	MMI3	MMI4
Alexandria, Va.	−77.044	38.812	3.5	3.5	3.0	3.0
Augusta, Ga.	−81.994	33.470	4.0	4.5	4.0	5.0
Augusta, Ky.	−84.002	38.769	3.5	4.0	4.0	NA
Baltimore, Md.	−76.626	39.287	3.0	3.0	4.5	3.0
Beaufort, S. C.	−80.670	32.432	6.0	6.0	6.0	6.0
Brownsville, Ohio	−82.256	39.946	4.5	4.5	3.0	5.0
Brownsville, Pa.	−79.884	40.024	5.0	4.0	4.5	5.0
Cape Girardeau, Mo.	−89.418	37.306	6.0	7.5	NA	8.0
Charleston, S. C.	−79.940	32.798	5.0	6.0	5.0	5.0
Chillicothe, Ohio	−82.985	39.330	F	6.5	6.0	6.0
Cincinnati, Ohio	−84.517	39.103	5.5	6.5	6.5	7.0
Circleville, Ohio	−82.949	39.594	5.0	6.0	6.0	6.0
Columbia, S. C.	−81.040	34.000	6.0	6.5	6.5	6.0
Dayton, Ohio	−84.188	39.739	5.0	6.0	5.0	5.0
Ft. Wayne, Ind.	−85.150	41.051	F	F	F	5.0
Frankfort, Ky.	−84.873	38.201	NA	7.5	6.0	6.0
Fredericksburg	−77.461	38.303	5.0	5.0	NA	4.0
Georgetown, S. C.	−79.308	33.382	5.0	5.0	5.0	4.0
Germantown, Pa.	−75.180	40.043	3.0	3.0	3.0	2.0
Hodgenville, Ky.	−85.740	37.574	4.0	5.0+	4.5	5.0
Knoxville, Tenn.	−83.920	35.978	4.0	4.5	5.0	NA
Lancaster, Pa.	−76.30	40.04	4.5	5.5	5.5	6.0
Lexington, Ky.	−84.508	38.041	5.5	6.5	6.5	6.0
Livingston City	−88.330	37.220	3.0	4.0	NA	5.0
Louisville, Ky.	−85.777	38.251	6.5	7.5	6.5	6.0
Marietta, Ohio	−81.455	39.417	4.0	5.5	4.5	4.0
Maysville, Ohio	−83.744	38.636	5.0	7.0	NA	6.0
Nashville, Tenn.	−88.786	36.162	6.5	7.5	7.0	6.0
New Haven, Conn.	−72.930	41.304	3.0	4.0	NA	2.0
New Orleans, La.	−90.069	29.971	3.5	5.0	4.0	4.0
New York, N. Y.	−73.996	40.728	3.0	4.5	4.0	4.0
Philadelphia, Pa.	−75.164	39.952	4.0	4.5	4.0	3.0
Pinckneyville	−81.468	34.843	4.0	4.5	4.0	5.0
Pittsburgh, Pa.	−79.983	40.440	5.0	5.0	4.0	5.0
Raleigh, N. C.	−78.647	35.791	3.0	F	4.0	5.0
Richmond, Va.	−77.480	37.550	5.5	5.5	6.5	5.0
Saint Louis, Mo.	−90.217	38.631	7.0	7.5	7.0	7.0
Savannah, Ga.	−81.091	32.064	5.5	6.0	NA	5.0
South Union	−86.657	36.876	F	F	4.0	6.0
Troy, Ohio	−84.203	40.039	4.0	5.0	4.5	6.0
Vincennes, Ind.	−87.525	38.679	6.0	6.5	6.5	6.0
Washington, D.C.	−77.026	38.891	4.5	4.5	5.5	4.0
Wheeling, W. Va.	−80.721	40.064	6.0	6.5	6.0	6.0
Worthington, Ohio	−83.018	40.093	4.0	4.5	4.0	4.0
Zanesville, Ohio	−82.013	39.94	4.5	5.5	4.5	5.0

follows identically the approach, and the analysis method, of that employed by *Bakun et al.* [2003] and *Bakun and Hopper* [2004]. That is, the extent to which the results differ will be a purely a consequence of the differences in intensity values.

[14] Any application of the *Bakun and Wentworth* [1997] method requires a regional intensity attenuation relation developed using instrumentally recorded calibration events. Ideally, the intensity values for calibration events should be reinterpreted following the same procedure as done in this study for the principal 1811–1812 events. In practice, however, such an effort is rarely if ever undertaken. Moreover, for the CEUS, the intensity attenuation relations are largely if not entirely constrained by low-to-moderate intensity values, including values from moderate earthquakes and intensities at regional distances for the 1929 Grand Banks earthquake. In a careful comparison of intensities determined for the 2001 Bhuj, India, earthquake from media reports and values from intensive ground surveys, *Hough and Pande* [2007] show that the tendency to infer inflated intensity values is significantly stronger for higher intensities (VI and above) than for weaker shaking levels.

[15] For NM1, NM1A, and NM3 we constrain the locations on the basis of lines of evidence that all three events occurred in the New Madrid Seismic Zone: NM1 on the Cottonwood Grove fault [see *Johnston and Schweig*, 1996], NM1A on either a northern segment of the Cottonwood Grove fault [*Johnston and Schweig*, 1996] or a southeast segment of the Reelfoot fault [*Mueller et al.*, 2004], and NM3 on the Reelfoot fault [e.g., *Johnston and Schweig*, 1996] (see Figure 5). The evidence for the rupture scenario for NM3 is particularly compelling, in particular, the waterfalls that formed where the fault crosses the Mississippi River [*Odum et al.*, 1998; *Johnston and Schweig*, 1996]. For NM2 we calculate a magnitude assuming a location on the northern limb of the NMSZ. Given the possibility that this event occurred outside of the NMSZ [*Mueller et al.*, 2004; *Hough et al.*, 2005], we also consider locations outside of the NMSZ.

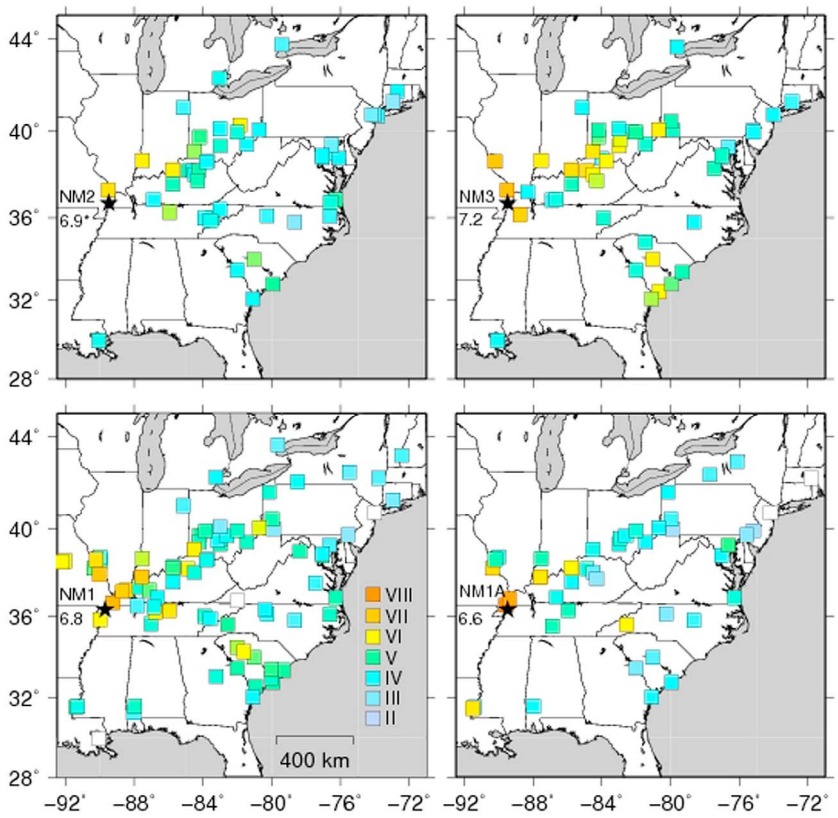

Figure 1. Consensus intensity values for NM2, NM3, NM1, and NM1A. The same length scale and color scale for modified Mercalli (MMI) values, shown in Figure 1 (bottom left), are used for all maps. The magnitude estimates correspond to the average of the results using the two attenuation models (see text). Stars indicate assumed location; for NM2, magnitude corresponds to assumed New Madrid Seismic Zone (NMSZ) location.

[16] For NM1 and NM1A we infer magnitude estimates of 6.7/6.9 and 6.5/6.7, respectively. The magnitude pairs are calculated using models 1 and 3, respectively; for large events the latter consistently yields higher values. For NM3 we estimate magnitudes of 7.1/7.3. The magnitude estimate of NM2 depends on the location of the event. Assuming the conventional NMSZ location we estimate magnitude values of 6.8/7.0. If the location is not constrained, the grid solution approach prefers locations several hundred km north/northeast of the NMSZ, but the location is very poorly constrained. For all plausible locations north/northeast of the NMSZ, the corresponding magnitude is lower than if one assumes a NMSZ location. For illustration, if we assume the location of the 1968 southern Illinois earthquake (37.96°N, −88.46°W), the magnitude estimates are lowered significantly, to 6.5/6.7. This location corresponds to the source zone proposed by *Mueller et al.* [2004] and *Hough et al.* [2005], a location along the Wabash River in southern Illinois where a detailed eyewitness account documents significant liquefaction. It is also close to the U.S. Saline, a site of natural salt springs and early salt production in southern Illinois that one of the most astute eyewitnesses to the sequence notes was the focus of continuing earthquake activity in the years following 1812 [*Drake*, 1815].

[17] *Bakun and Hopper* [2004] estimate magnitude values of 7.6, 7.5, and 7.8 for NM1, NM2, and NM3, respectively, using attenuation model 3. Their 95% confidence ranges do overlap with the values estimated in this study: 6.8–7.9, 6.8–7.8, and 7.0–8.1 for NM1, NM2, and NM3, respectively. The magnitudes for NM1, NM2, and NM3 estimated by *Hough et al.* [2000] are also higher than those determined in this study: 7.2–7.3, 7.0, and 7.4–7.5 for NM1, NM2, and NM3, respectively. *Hough et al.* [2000] use the isoseismal method of *Johnston* [1996a] to determine magnitude values. Using the *Bakun and Wentworth* [1997] method with the intensity values of *Hough et al.* [2000] and both models 1 and 3, one estimates 7.0/7.3 for NM1, 7.0/7.1 for NM2 assuming a NMSZ location, and 7.4/7.7 for NM3.

[18] One can consider the intensity distributions determined by each of the individual experts (Figure 4). For this calculation, we use only the intensity values from each expert from locations for which we calculated a consensus intensity values. That is, we do not include intensity values determined by individual experts if either no or only one other expert assigned an intensity for that account.

[19] The assignments by individual experts reveal no glaring overall biases (see Figure 2). Further, while there is a tendency for individual experts to have generally high or low assignments for all events, the biases are not entirely systematic. For example, the lowest magnitude for NM1 and the highest magnitude for NM1A correspond to assignments from the same expert. The individual assignments for NM1 yield magnitude values as low as 6.69/6.85 and as high as 6.85/7.08. For NM2 the estimates range from 6.72/6.86 to

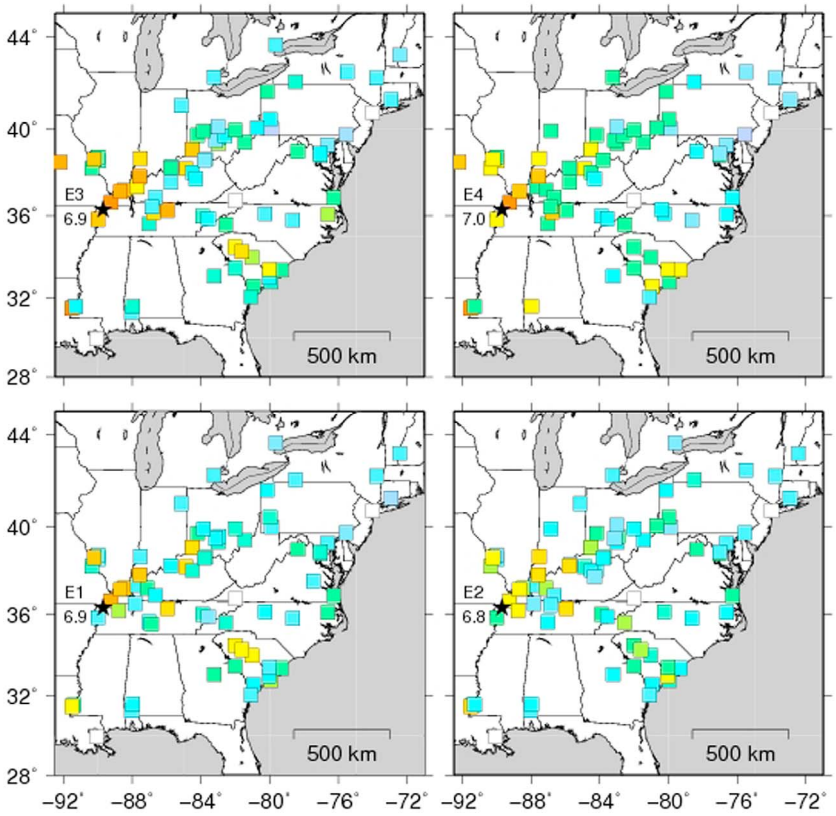

Figure 2. Intensity assignments for NM1 from the four individual experts. The magnitude estimates are the average from the two attenuation models (see text).

6.91/7.09. For NM3, the estimates range from a low of 6.83/7.02 to 7.21/7.50. The largest spread is found for NM1A: 6.31/6.35 to 6.67/6.85. The large spread for NM1A reflects a greater degree of variability of intensity assignments between the four experts. The accounts of this event are especially sparse and fragmentary. Further, the intensity assignments for a small number of near-field accounts of strong shaking are especially variable.

[20] The variation in magnitude estimates is typically on the order of 0.1–0.3 units, although values close to 0.5 units are found for NM3 as well as NM1A. We define δM values for each event, expert, and attenuation model as the difference between each magnitude estimate and the lowest for a given event and attenuation model (Figure 4). For each event, the minimum δM is zero. Considering only the three main shocks, Figure 4 reveals a correlation between δM and $M_{\min}$: δM is both larger and more variable for a given event for larger $M_{\min}$ values.

[21] The uncertainties associated with the individual intensity assignments are independent from those associated with the attenuation relation. Thus, for example, the range of estimates for event NM3, not considering the formal uncertainties of the grid search method, is 6.8–7.5 (Figure 4). For NM1, the range of estimates is 6.7–7.1.

[22] The grid search analysis indicates the range in magnitude estimates corresponding to location uncertainties, for a given attenuation model. For NM1, this range, using model 1 and assuming a location on the Cottonwood Grove fault, is roughly 6.7–6.8. For NM3, magnitude values vary by less than 0.1 units for any assumed epicenter along the Reelfoot fault (Figure 5).

[23] *Bakun and Hopper* [2004] present several reasons why they consider model 3 to be preferred to model 1.

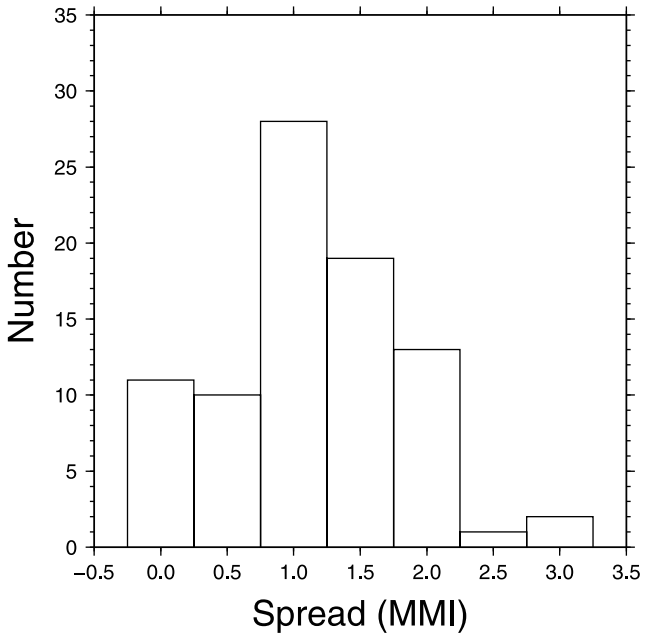

Figure 3. The spread of individual intensity assignments for NM1.

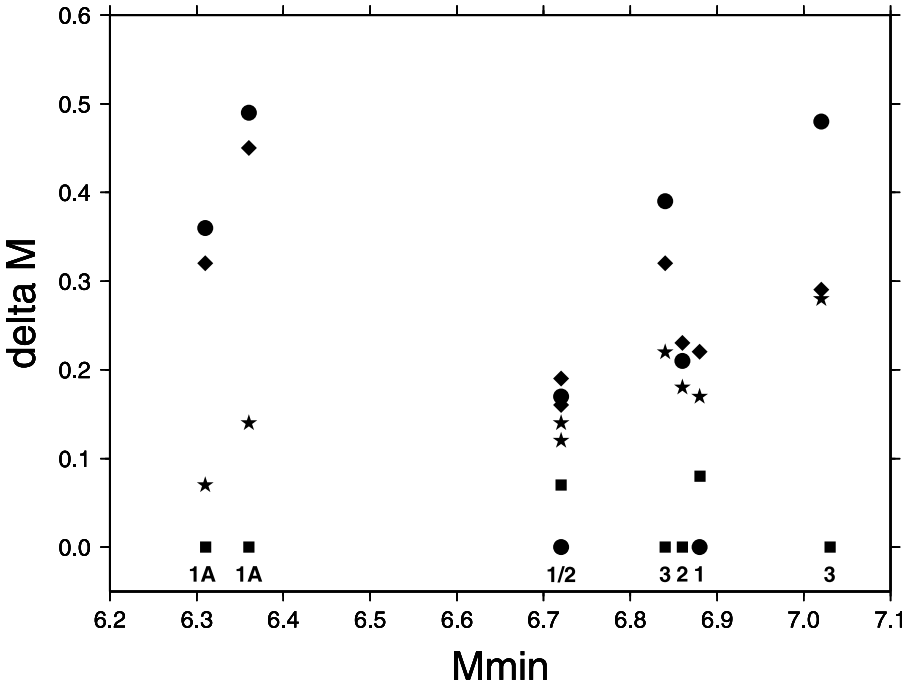

Figure 4. The range of magnitude values inferred from the individual expert assignments versus the minimum magnitude for that event. Different symbols correspond to δM results for each expert. For each of eight event/attenuation model pairs, the minimum δM is zero, corresponding to the lowest of the estimates from the four experts; three additional values reflect the arithmetic difference between this minimum and the other estimates. Numbers along bottom refer to event: 1A for NM1A, etc. For each event, the lower of two estimates corresponds to attenuation model 1.

However, as discussed by *Bakun and Hopper* [2004], attenuation relations for CEUS are constrained almost entirely from $M < 6$ calibration events. This fundamental data limitation has plagued every investigation of New Madrid magnitudes dating back to the seminal study by *Nuttli* [1973] and is apparent from the significant differences in magnitude values obtained with the two attenuation models. Morever, *Szeliga et al.* [2010] present evidence that the *Bakun and Wentworth* [1997] method is fundamentally unstable when used to analyze large intraplate earthquakes. They show, for example, that even using an attenuation relation for cratonic India that is constrained by intensities from the 2001 M_w7.6 Bhuj, India, earthquake, the method significantly overestimates the magnitude of the event (M8 versus M7.6). In light of these limitations we suggest that any analytical method and/or specific intensity attenuation relation can at best provide an indication of the magnitudes that are consistent with the observations.

[24] We note that no attempt is made in this study to consider site response. The issue of site response, and site corrections, in intensity studies is problematic because every set of intensity values include a subset that reflect site amplifications. One cannot simply apply site corrections to a target historical earthquake if no such corrections are made for intensity values for the calibration earthquakes. However, as discussed by *Hough et al.* [2000], the intensity distributions for the principal 1811–1812 earthquakes are systematically biased owing to early settlement patterns, in particular the concentration of early settlers immediately along the major river valleys. As discussed at length by *Hough et al.* [2000], although population centers in the midcontinent remained concentrated along waterways as the population grew, settlements quickly moved away from immediate riverbanks with the advent of efficient land transportation. If one analyzes the intensity values without consideration of this factor, as we have done here, it is possible if not likely that the magnitude estimates will be biased high by an amount that is difficult to estimate. On the basis of the arguments presented by *Hough et al.* [2000], this bias is potentially significant.

[25] A final consideration concerns sampling. Comparing consensus MMI values for NM1 and NM3 (Figure 6), we find considerable overlap between the two sets of values at distances less than ~700 km, but that values for NM3 are systematically higher at greater distances. As noted, the number of intensity values for NM3 is only about half the number available for NM1. The more sparse archival record appears to be at odds with the conclusion that NM3 was the largest event in the sequence. It is possible that, by the time of this event, earthquakes were viewed as less newsworthy by eyewitnesses who had experienced an active sequence, with multiple main shocks and large aftershocks. However, considering Figure 4, another plausible interpretation is that the difference between the two distributions stems largely from the absence of low MMI values (or "not felt" reports) for NM3. This highlights a general sampling issue with analysis of macroseismic data: for sparse historical intensity sets especially, reliable "not felt" reports are likely to be

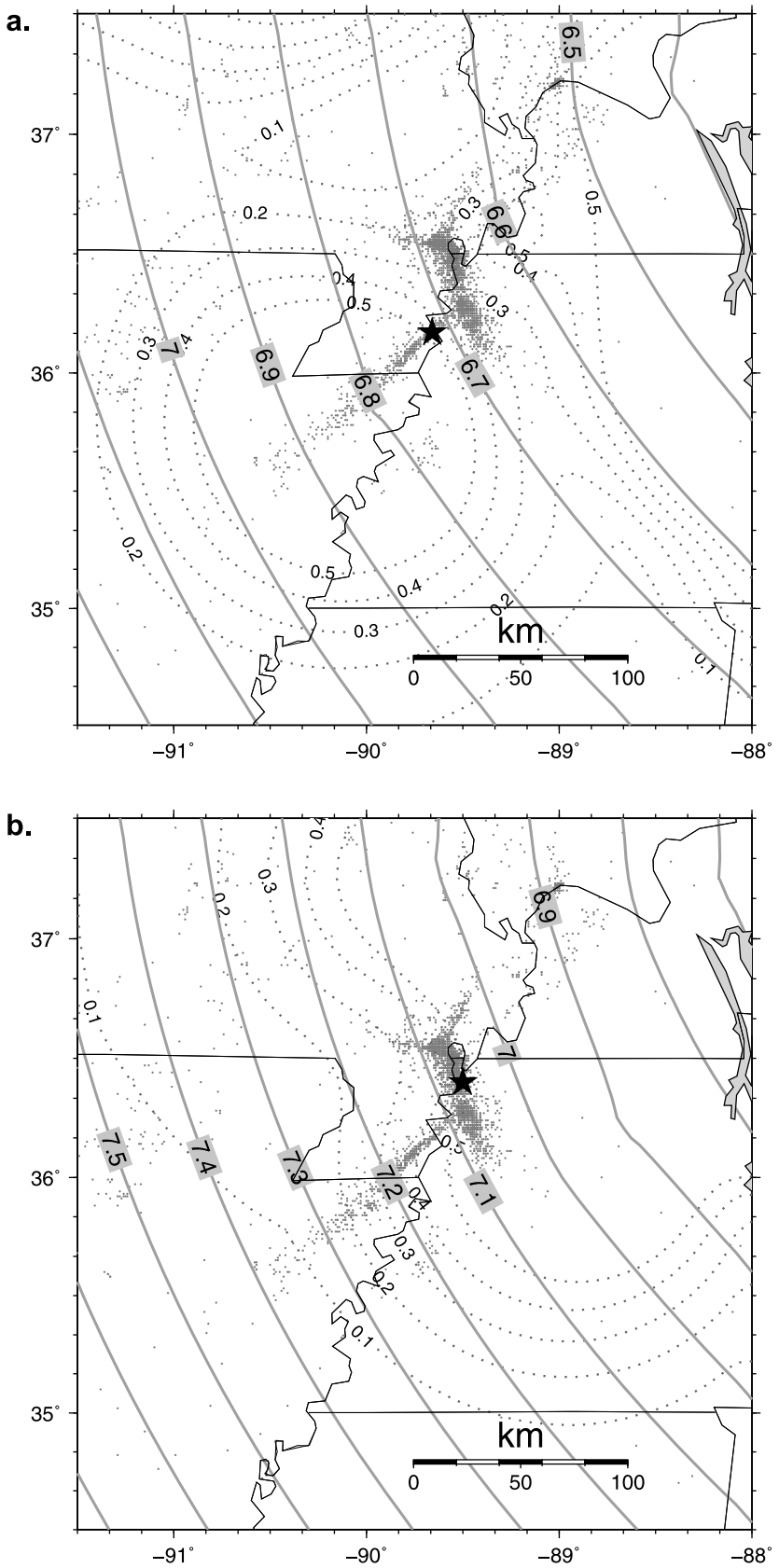

Figure 5. (a) Contoured RMS and magnitude values corresponding to trial grid of epicenters for NM1. Star indicates the assumed epicenter along the Cottonwood Grove fault, assumed to be illuminated by instrumentally recorded microseismicity (small circles). (b) Same as Figure 5a but for NM3. The central band of microseismicity in the NMSZ illuminates the Reelfoot fault.

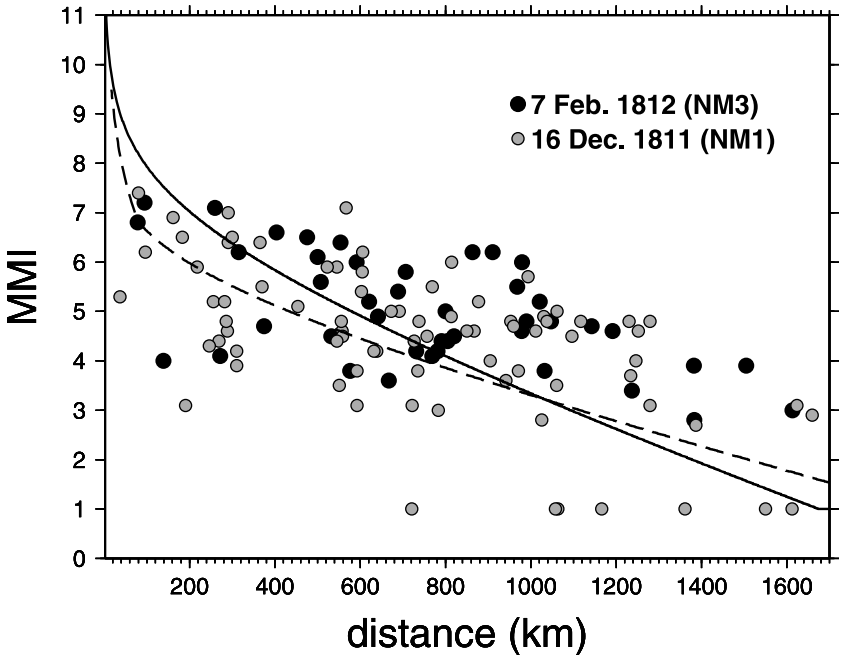

Figure 6. Intensity values for NM1 (gray circles) and NM3 (black circles), predicted MMI(r) for *M*7.0 using attenuation model 1 (solid line), and predicted line for *M*7.0 using attenuation relation of *Atkinson and Wald* [2007] (dashed line).

lacking, and weakly felt shaking is less likely than stronger shaking to be reported. This leads to an oversampling of sites with relatively high intensity values at regional distances. This bias is expected to persist for more recent events as well, including the calibration events used to determine attenuation relations. However, the bias is expected to be especially severe for the earliest events, for which available archival accounts are especially sparse.

4. Consistency With Scaling Relations

[26] Estimating preferred magnitudes for the four principal earthquakes by taking an average of the results from the two attenuation relations using the consensus intensities, one infers values of 6.8, 6.6, and 7,2 for NM1, NM1A, and NM3, respectively, and 6.9 for NM2 assuming a NMSZ location. All of these values are considerably lower than previously published magnitude values estimated using macroseismic data [e.g., *Nuttli*, 1973; *Johnston*, 1996b; *Newman et al.*, 1999; *Hough et al.*, 2000; *Bakun and Hopper*, 2004] (Figure 7). Values approaching those estimated by *Hough et al.* [2000], 7.25, 7.1, and 7.45 for NM1, NM2, and NM3, respectively, are within the uncertainty ranges associated with intensity and attenuation relation uncertainties, in particular if one considers the highest individual intensity assignments and the attenuation relation (model 3) that yields higher magnitudes (e.g., Figure 4). Thus, while the results do not rule out the magnitude values estimated by *Hough et al.* [2000], they do not, considered in aggregate, support values this high, let alone higher values.

[27] Considering the preferred as well as the lower bound estimates inferred in this study, one can ask the question, are these results consistent with other lines of direct and indirect evidence? We first consider whether they are consistent with published scaling relations. Scaling relations established from earthquakes with well-documented ruptures [e.g., *Wells and Coppersmith*, 1994] provide only a weak constraint on earthquake magnitudes for historical events, in particular when rupture parameters are not well constrained. For this discussion we focus on NM3 for two reasons: (1) according to our results as well as those of *Hough et al.* [2000], it was the largest event in the 1811–1812 sequence, and (2) it is the event for which we have the best constraint on rupture parameters.

[28] The most compelling evidence that NM3 occurred on the Reelfoot fault are the eyewitness accounts of waterfalls that were created along the Mississippi River by this event, accounts that suggest a riverbed uplift on the order of 1 m to several meters [see *Johnston and Schweig*, 1996; *Odum et al.*, 1998]. The association of NM3 with the Reelfoot fault implies that this event, perhaps along with NM1A [see *Hough and Martin*, 2002], was responsible for the creation of Reelfoot Lake. Recent investigations [e.g., *Champion et al.*, 2001] have identified and characterized the Reelfoot scarp, interpreting the scarp not as primary surface rupture but as a fold limb. *Champion et al.* [2001] conclude that the fault tip terminates at a depth of approximately 500–1000 m below the surface. We assume, given the tightness of the flexure and the fact that the rupture nearly reached the surface, that the surface offset inferred from the waterfall observations provides a reasonable indication of surface slip.

[29] If we assume that NM3 ruptured from near the town of New Madrid (i.e., one of the documented waterfall locations) to the edge of Reelfoot Lake, this implies a rupture length of approximately 30–40 km. Significantly longer rupture lengths, as much as 100 km, have been inferred by other studies [e.g., *Johnston and Schweig*, 1996] based

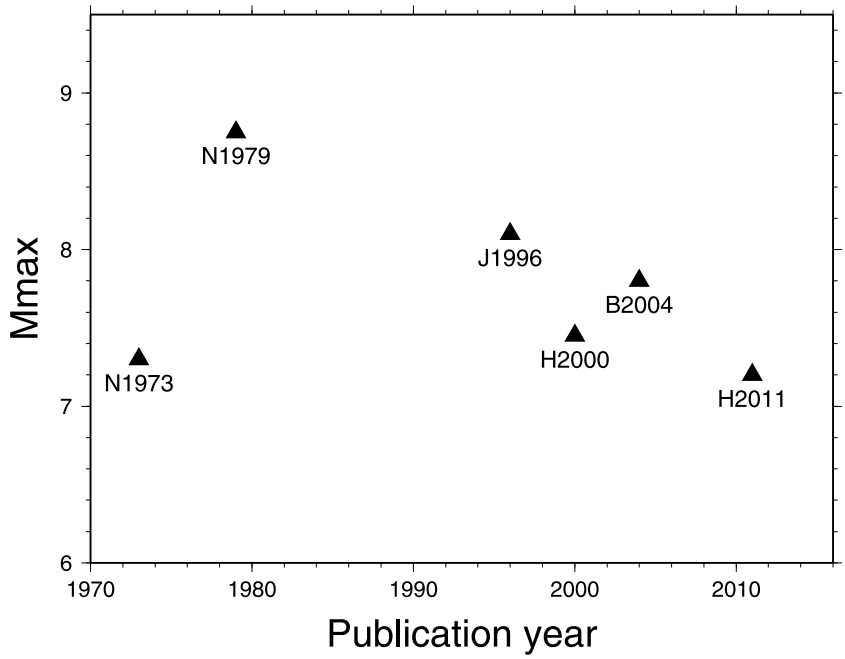

Figure 7. Magnitude estimate of largest 1811–1812 main shock as a function of publication year: N1973, *Nuttli* [1973]; N1979, *Nuttli* [1979]; J1996, *Johnston* [1996b]; H2000, *Hough et al.* [2000]; B2004, *Bakun and Hopper* [2004]; H2011, this study. The M_{max} value estimated by *Nuttli* [1979] was never published in the peer-reviewed literature but was the basis for the widely quoted assertion that the New Madrid earthquakes were the biggest events ever witnessed in the contiguous United States.

primarily on the extent of ongoing microseismicity, which is generally assumed to be a continuing aftershock sequence and therefore to illuminate the extent of the historic ruptures. However, *Mueller et al.* [2004] show that side limbs of NMSZ activity are consistent, assuming aftershock triggering by static stress change, with side lobes of increased stress associated with a 35–40 km rupture of the central Reelfoot fault. Further, as noted by *Mueller et al.* [2004], an extension of thrust faulting on the Reelfoot fault to the S-SE of the junction with the strike-slip Cottonwood Grove fault is kinematically inconsistent. We therefore take 35 km as a plausible lower bound (if not the preferred estimate) for rupture length. The width of the NM3 rupture has been similarly debated. Although one can appeal to arguments that the rupture extended deeper, we suggest that the depth of microseismicity (15 km [e.g., *Odum et al.*, 1998; *Mueller and Pujol*, 2001]) provides a plausible lower bound for the downdip rupture length.

[30] Taking plausible lower bounds for the rupture parameters to be 35 km length, 22 km width [*Mueller and Pujol*, 2001], and 1 m average slip, and assuming shear modulus of 3.3×10^{11} dyn cm, implies M_w6.9. Alternatively, using either the rupture length-magnitude or the area-magnitude scaling relations of *Wells and Coppersmith* [1994] for reverse events in California, one infers a value of M_w6.8.

[31] One might equally well ask if the higher-magnitude estimates are consistent with established scaling relations. For example, if one fully doubles each of the rupture length, width, and average slip values, the magnitude increases to M_w7.4. Although arguments have been advanced that coseismic slip could extend well below the seismogenic depths as illuminated by microseismicity [e.g., *Johnston and Schweig*, 1996], we suggest the doubled values are less generally plausible than the values considered above.

5. Consistency With Liquefaction Observations

[32] As documented originally by *Fuller* [1912], the 1811–1812 New Madrid sequence generated widespread liquefaction throughout the New Madrid Seismic Zone. Sand-blow deposits cover over 1% of the ground surface over a swath approximately 230 km × 60 km [*Obermeier*, 1989]. Both the extent and the size of liquefaction features provide some constraint on magnitude, although with significant uncertainty for large intraplate earthquakes in particular [e.g., *Obermeier et al.*, 1993; *Tuttle and Schweig*, 1996]. For example, shallow crustal earthquakes as small as *M*6.5 and as large as 7.8 have generated liquefaction out to 100 km [e.g., *Obermeier et al.*, 1993].

[33] In addition to the limitations of calibration relations, the 1811–1812 sequence, unlike the 2001 Bhuj, India, earthquake to which it has been compared [e.g., *Tuttle et al.*, 2002], comprised four large events distributed over at least two, and possibly more, distinct faults. Comparing the swath of significant liquefaction with the rupture scenario proposed by *Mueller et al.* [2004], for example, the maximum distance of significant liquefaction from the nearest fault rupture is less than 50 km. If the magnitudes are somewhat smaller than the values inferred by *Mueller et al.* [2004], and the rupture lengths correspondingly shorter, the entire zone of significant liquefaction would still be at most 80 km from the nearest fault rupture. As a further note, although liquefaction north of the Reelfoot fault has been interpreted as evidence for primary main shock rupture on the northern

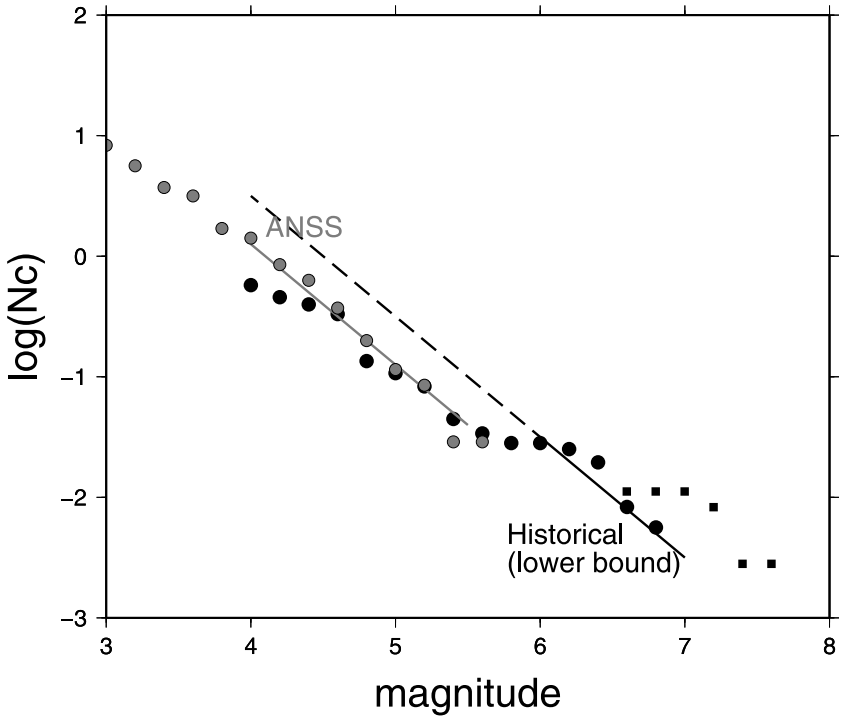

Figure 8. The cumulative number of earthquakes per year equal to or larger than a given magnitude, shown for the greater NMSZ region using the modern instrumental (Advanced National Seismic System, ANSS) catalog (gray circles) and historic magnitude values using both the lower bound estimates (large black circles) and upper bound estimates (black squares) for events analyzed in this study. Lines indicate *b* values of 1, fit by eye for illustration.

limb of the New Madrid Seismic Zone [e.g., *Johnston and Schweig*, 1996], this zone also extends no farther than 50 km from the Reelfoot fault. Thus, while the extent and size of liquefaction features created during the 1811–1812 sequence supports the inference of large earthquakes, the observations cannot constrain the magnitudes within the range of values discussed in this paper. In particular they cannot rule out values as low as our preferred estimates.

6. Long-Term Magnitude Distribution

[34] One can revisit the long-term distribution of NMSZ magnitudes given the magnitude estimates determined by this study as well as revised magnitudes for several large aftershocks of the 1811–1812 sequence [*Hough*, 2009]. For the large events, the uncertainties associated with intensity assignments and the attenuation relation are generally dependent between events. Thus, if we define the preferred estimates to be the magnitudes determined using the consensus intensities and the average result using the two attenuation models, it is possible that these estimates are systematically biased for all events.

[35] We thus consider the cumulative rate of earthquakes for the greater NMSZ, defined to be bounded between 33° and 40°N, −94° and −85°W, using both the high and the low estimated magnitude estimates. For this calculation we use a region larger than the NMSZ as traditionally defined. This is based on results indicating that the sphere of influence of NMSZ earthquakes, for example as revealed by the distribution of ongoing microseismicity–commonly interpreted as long-lived aftershocks [e.g., *Ebel et al.*, 2000; *Stein and Liu*, 2009]–extended to considerable distance [e.g., *Hough*, 2001]. We determine a rate of events separately using the historic catalog [*Seeber and Armbruster*, 1991], which covers 1627–1985, and the modern instrumental catalog for 1974–2009. The historic catalog is updated to include the results of this study as well as the additional 1811–1812 aftershocks and triggered earthquakes analyzed by *Hough* [2009]. Figure 8 presents the magnitude distribution for the combined instrumental and historical catalogs.

[36] Figure 8 reveals no evidence for a clear bump at a particular characteristic magnitude, but rather a GR distribution, with a *b* value not indistinguishable from 1, between roughly *M*6 and *M*7–7.5. Although the historical catalog includes small and moderate earthquakes, it is not expected to be complete, in particular during the early historical record, for moderate magnitudes. The apparent departure from a *b* value distribution for magnitudes below 6 is thus not considered robust.

[37] The aggregate magnitude distribution is similar to that obtained by combining available catalogs (instrumental, historic, prehistoric) in California [*Page et al.*, 2008]. We also find an offset in *a* value between the instrumental and the historic catalogs, roughly a factor of 2.5. *Page et al.* [2008] show that, assuming standard ETAS clustering statistics [e.g., *Felzer et al.*, 2002], a short catalog will tend to underestimate the long-term *a* value because of the tendency for significant events, and their aftershocks, to cluster. Whether or not this bias can account for the factor of 2.5 discrepancy is not clear. An alternative interpretation is that

CEUS seismicity is characterized by significant rate changes over timescales of decades to centuries.

7. Predicted Moment Release Rate

[38] We now consider the predicted rate of moment release assuming that NMSZ strain is generated by postglacial rebound. Although other models have been proposed to explain Holocene NMSZ activity [e.g., *Calais et al.*, 2010], we focus on postglacial rebound because it can successfully account for Holocene activity along the St. Lawrence Seaway [*Mazzotti et al.*, 2005]. Considering first the general predictions of modeling of postglacial rebound, *Wu and Johnston* [2000, p. 1325] conclude that the mechanism is "unlikely to have triggered the large M8 earthquakes in New Madrid." This conclusion, however, is in large part based on the assumption that the 1811–1812 sequence involved significant moment release on strike-slip faults. The modeling of *Wu and Johnston* [2000] predicts a predominantly thrust mode of failure for NMSZ earthquakes associated with postglacial rebound. The results of our study, in contrast to a number of earlier studies [e.g., *Johnston*, 1996b], do indicate that moment release in the sequence was predominantly associated with thrust faulting.

[39] We can further consider the strain rate predicted to be associated with postglacial rebound. *Anderson* [1979] shows that seismic strain rate, $d\varepsilon/dt$, for an areal zone can be estimated:

$$d\varepsilon/dt = (dM_o/dt)/(2.67\mu Ah), \quad (1)$$

where dM_o/dt is the moment rate, μ is the shear modulus (taken as 3.3×10^{11} dyn cm^2), A is the area of the seismic zone, and h is its thickness. Following *Anderson* [1986], we assume a constant h of 15 km. Given the values of $d\varepsilon/dt$ (10^{-9}/yr) and A (20,000–40,000 km^2 inferred by *Grollimund and Zoback* [2001]) [see also *Anderson*, 1986], equation (1) yields $dM_o/dt = 2.6$–5.3×10^{23} dyn cm/yr. The modeling of *Grollimund and Zoback* [2001] further predicts that the strain rate has been nearly constant through most of the Holocene, and will remain nearly constant for at least the next 10,000 years. One can thus consider models that are essentially steady state over tens of ka timescales.

[40] If we assume for simplicity that the corresponding Holocene moment release will be accounted for by earthquakes with a Gutenberg-Richter distribution [*Gutenberg and Richter*, 1944] truncated at $M_{\max}$, events within 0.2 units of the $M_{\max}$ events will account for 72% of the moment release. We thus estimate

$$dM_o/dt = 1.4M_{o,\max}/t_r, \quad (2)$$

where t_r is the average recurrence rate and $M_{o,\max}$ is the moment of the $M_{\max}$ events. If we assume t_r = 500 years (the approximate recurrence of documented late Holocene sequences [see *Tuttle et al.*, 2002]), equation (2) yields $M_{\max}$ = 6.6–6.8. Alternatively, one can assume a longer average recurrence rate and a larger $M_{\max}$. For example, if we assume t_r = 1000 years, equation (2) yields $M_{\max}$ = 6.8–7.0.

[41] A steady state model with t_r > 500 years can be consistent with observed late Holocene clustering, in particular if, given the expected variability of recurrence time, the probability of observing the clustering is not unduly low. To explore such models, we generate two random sequences of $M_{\max}$ events, one in which $M_{\max}$ events have a specified recurrence with a normal distribution and a coefficient of variation (COV) of 0.5 (the lowest reasonable value), and one with a Poissonian recurrence rate (COV = 1). In generating the random sequences, when the predicted interval is less than zero, we set the interval to zero. (The estimated probabilities differ slightly if we set negative values to 50, or exclude them.) We then ask, given that a historical sequence occurred in 1811–1812, what is the probability, for both models and different assumed values of t_r, that 3 sequences would have been observed over the preceding 1000 years.

[42] Table 5 reveals that assuming a Poissonian rate, the probability of observing late Holocene clustering by random chance is reasonably high (>15%) for t_r values as high as 1500 years, and 26% for Poissonian recurrence and t_r = 1000 years. We note that t_r = 1000 years is close to the average rate that would be inferred given 6 events between 2350 B.C. and the present time, assuming the record established from paleoliquefaction is complete.

[43] Regarding the mode of failure predicted by postglacial rebound, *Wu and Johnston* [2000] conclude that postglacial rebound will generate a thrust failure mode in the NMSZ. Although the magnitude estimates from this study are lower than those estimated by *Hough et al.* [2000], in both studies NM3 is estimated to have been the largest event in the sequence. *Hough and Martin* [2002] further present evidence that NM1A was also a thrust event on a segment of the Reelfoot fault.

8. Discussion and Conclusions

[44] The predicted postglacial rebound strain rate estimated by *Grollimund and Zoback* [2001] is sufficient to produce moderately large earthquakes, on the order of M_w6.8, every 500 years, or somewhat larger earthquakes, on the order of low M_w7.0, that recur on average less frequently than the observed rate of late Holocene NMSZ sequences. A model with an average recurrence time as high as 1500 years, with $M_{\max}$ events close to M_w7, and a Poissonian distribution of $M_{\max}$ events, is considered plausible. That is, such a model is expected to produce the observed late Holocene clustering infrequently, but with a high enough probability that it could plausibly have occurred by random chance.

[45] Predicted postglacial strain rates are thus sufficient to produce earthquakes with magnitude and recurrence rates comparable to the results of our consensus intensity analysis. We note that, in comparing the predicted moment release rate with observations, one complication is the fact that each of the historic and prehistoric sequences comprised multiple large main shocks. It is thus appropriate to consider each sequence in terms of equivalent overall moment release. The "low bid" estimates for NM1, NM1A, NM2, and NM3, not including site response or sampling biases, are 6.7, 6.3, 6.5, and 6.8, which yields an overall moment release equivalent to one M7.0 event.

[46] As discussed by other studies [e.g., *Grollimund and Zoback*, 2001; *Calais et al.*, 2006], postglacial strain cannot account for NMSZ seismic activity if the 1811–1812 and earlier sequences involved one or more earthquakes as large as or larger than M_w7.5. However, the size of the

Table 5. Candidate Models for M_{max} Average Recurrence[a]

t_r (years)	COV	M_{max}	P (3 < 1000 years)
500	0.5	6.6–6.8	49%
500	1.0	6.6–6.8	59%
750	0.5	6.7–6.9	17%
750	1.0	6.7–6.9	38%
1000	0.5	6.8–7.0	7.4%
1000	1.0	6.8–7.0	26%
1500	0.5	6.9–7.1	2.4%
1500	1.0	6.9–7.1	15%
1800	0.5	7.0–7.2	1.4%
1800	1.0	7.0–7.2	11%

[a]The probability of observing three sequences during the 1000 years prior to 1811–1812 by random chance assuming models with prescribed repeat time, t_r, of M_{max} events, and a coefficient of variation (COV) of 0.5 or 1.0.

principal 1811–1812 events has been the subject of enormous debate, with published estimates ranging over at least a full magnitude unit. The grid search method of *Bakun and Wentworth* [1997], combined with carefully considered intensity values, provides the basis for systematic, objective analysis of magnitudes. In this study we have attempted to consider the full uncertainties associated with application of the method in the central/eastern U.S. Although previous studies have reported uncertainties based on the residuals to the least squares fit, this formal measure does not consider two additional sources of uncertainty: that associated with the attenuation relation and that associated with the intensity values. Our results reveal that, for the four principal 1811–1812 earthquakes, uncertainties in the intensity values themselves give rise to magnitude uncertainties on the order of 0.2–0.3 units.

[47] Although we do not formally explore the uncertainty associated with the attenuation relation, the different results that are obtained using the two CEUS attenuation relations is useful for illustration. These two relations are based on the same set of intensity values, differing only in the mathematical approach to extrapolation. For the events analyzed here, the two relations yield magnitude estimates that differ by 0.2–0.3 units. Issues such as these highlight the need for caution in the application of the *Bakun and Wentworth* [1997] approach, in particular for the analysis of large historical earthquakes. These issues notwithstanding, analysis of consensus intensities for the four principal New Madrid earthquakes yields significant lower-magnitude values than those estimated by earlier studies. The uncertainty range moreover permits values as low as those shown in Figure 6, and potentially implies a much smaller discrepancy between rates inferred from the modern catalog and those inferred from the historical catalog.

[48] The magnitude uncertainty range inferred in this study further provides a basis for reconciling the observed strain release and predicted/observed strain accrual in the NMSZ. Regarding the spatial clustering of activity, postglacial rebound does not by itself provide an explanation for spatially concentrated strain release. The model of *Grollimund and Zoback* [2001], for example, includes a local zone of weakness associated with the inferred lower crustal mafic pillow. This zone of weakness concentrates strain within a zone upward of 20,000 km^2. Several studies [e.g., *Cox et al.*, 2001; *Mitchell et al.*, 2008; T. L. Pratt, Structural setting and long-term deformation of the New Madrid Seismic Zone, central U.S., submitted to Geology, 2010] have presented evidence for significant strain release outside the modern, central NMSZ. The model of *Grollimund and Zoback* [2001] is consistent with a migration of Holocene activity over distances of 100–200 km from the central NMSZ. The predicted rate of moment release corresponds to events occurring anywhere within the region of postglacial strain concentration. Attributing ongoing activity to postglacial rebound does, however, predict a predominantly thrust mode of failure.

[49] One cannot rule out alternative viable models for the NMSZ that involve larger maximum earthquakes and/or characteristic NMSZ earthquakes. The model of *Kenner and Segall* [2000], for example, illustrates how a sequence of large earthquakes on a buried fault could be associated with undetectable rates of present-day interseismic strain. However, we have shown that it is possible to construct more simple models for the NMSZ that reconcile a number of observations and results that have formerly appeared irreconcilable: (1) a strain rate controlled by postglacial rebound, (2) the absence of a resolvable observed strain rate, (3) the late Holocene clustering of sequences like 1811–1812, (4) a Gutenberg-Richter magnitude distribution for the greater NMSZ, and (5) magnitude estimates for the principal 1811–1812 events derived from analysis of macroseismic data, and supported by scaling relations. A range of such models, with varying M_{max} and t_r values can be constructed; all plausible models require M_{max} values that are lower than almost all previously published estimates, but permissible considering the uncertainties inferred in this study.

[50] **Acknowledgments.** The intensity assignments analyzed in this study were made by Duncan Agnew, Paola Albini, Kenneth Burke, and Stacey Martin. We thank Walter Szeliga, Tom Pratt, and two anonymous reviewers for constructive reviews of the manuscript, and Bill Bakun for providing his grid search code. We further acknowledge additional reviews from Rob Williams, Rus Wheeler, Jack Boatwright, Bill Bakun, Thomas Brocher, and Jeanne Hardebeck. Robert Nowack is gratefully acknowledged for editorial wisdom and patience. Figures were generated using GMT software [*Wessel and Smith*, 1999]. This work was supported by the U.S. Nuclear Regulatory Commission Office of Nuclear Regulatory Research Project N6501 RES-08-129. Any opinions, findings, and conclusions expressed in this material are those of the authors and do not necessarily reflect the views of the U.S. Nuclear Regulatory Commission and the U.S. Geological Survey.

References

Ambraseys, N. N. (1983), Notes on historical seismicity, *Bull. Seismol. Soc. Am.*, *73*, 1917–1920.

Ambraseys, N. N. (2006), Comparison of frequency of occurrence of earthquakes with slip rates from long-term seismicity data: The cases of Gulf of Corinth, Sea of Marmara, and Dead Sea Fault Zone, *Geophys. J. Int.*, *165*, 516–526, doi:10.1111/j.1365-246X.2006.02858.x.

Ambraseys, N., and R. Bilham (2003), Reevaluated intensities for the great Assam earthquake of 12 June 1897, Shillong, India, *Bull. Seismol. Soc. Am.*, *93*, 655–673, doi:10.1785/0120020093.

Anderson, J. G. (1979), Estimating the seismicity from geological structure for seismic risk studies, *Bull. Seismol. Soc. Am.*, *69*, 135–158.

Anderson, J. G. (1986), Seismic strain rates in the central and eastern United States, *Bull. Seismol. Soc. Am.*, *76*, 273–290.

Atkinson, G. M., and D. J. Wald (2007), "Did You Feel It?" intensity data: A surprisingly good measure of earthquake ground motion, *Seismol. Res. Lett.*, *78*, 362–368, doi:10.1785/gssrl.78.3.362.

Bakun, W. H., and M. Hopper (2004), Magnitudes and locations of the 1811–1812 New Madrid, Missouri and the 1886 Charleston, South Carolina earthquakes, *Bull. Seismol. Soc. Am.*, *94*, 64–75, doi:10.1785/0120020122.

Bakun, W. H., and A. McGarr (2002), Differences in attenuation among the stable continental regions, *Geophys. Res. Lett.*, *29*(23), 2121, doi:10.1029/2002GL015457.

Bakun, W. H., and C. M. Wentworth (1997), Estimating earthquake location and magnitude from seismic intensity data, *Bull. Seismol. Soc. Am.*, *87*, 1502–1521.

Bakun, W. H., A. C. Johnston, and M. G. Hopper (2003), Estimating locations and magnitudes of earthquakes in eastern North America from modified Mercalli intensities, *Bull. Seismol. Soc. Am.*, *93*, 190–202, doi:10.1785/0120020087.

Bollinger, G. A. (1977), Reinterpretation of the intensity data for the 1866 Charleston, South Carolina, earthquake, *U.S. Geol. Surv. Prof. Pap.*, *1028-B*, 17–32.

Boyd, O. S., Y. Zeng, A. D. Frankel, and L. Ramirez-Guzman (2010), Crustal deformation modeling in the central United States (abstract), *Seismol. Res. Lett.*, *81*, 323.

Calais, E., and S. Stein (2009), Time-variable deformation in the New Madrid Seismic Zone, *Science*, *323*, 1442, doi:10.1126/science.1168122.

Calais, E., J. Y. Han, C. DeMets, and J. M. Nocquet (2006), Deformation of the North American plate interior from a decade of continuous GPS measurements, *J. Geophys. Res.*, *111*, B06402, doi:10.1029/2005JB004253.

Calais, E., A. M. Freed, R. Van Arsdale, and S. Stein (2010), Triggering of New Madrid seismicity by late-Pleistocene erosion, *Nature*, *466*, 608–611, doi:10.1038/nature09258.

Champion, J., K. Mueller, A. Tate, and M. Guccione (2001), Geometry, numerical models and revised slip rate for the Reelfoot fault and trishear fault-propagation fold, New Madrid Seismic Zone, *Eng. Geol. Amsterdam*, *62*, 31–49, doi:10.1016/S0013-7952(01)00048-5.

Cox, R. T., R. B. Van Arsdale, J. B. Harris, and D. Larsen (2001), Neotectonics of the Reelfoot rift zone margin, central United States, and implications for regional strain accommodation, *Geology*, *29*, 419–422, doi:10.1130/0091-7613(2001)029<0419:NOTSRR>2.0.CO;2.

Drake, D. (1815), *Natural and Statistical View, or Picture of Cincinnati and the Miami County, Illustrated by Maps*, Looker and Wallace, Cincinnati, Ohio.

Ebel, J., E. Bonjer, and M. Oncescu (2000), Paleoseismicity: Evidence for past large earthquakes, *Seismol. Res. Lett.*, *71*, 283–294.

Felzer, K. R., T. W. Becker, R. Abercrombie, G. Estrom, and J. R. Rice (2002), Triggering of the 1999 M_w7.1 Hector Mine earthquake by aftershocks of the 1992 M7.3 Landers earthquake, *J. Geophys. Res.*, *107*(B9), 2190, doi:10.1029/2001JB000911.

Fuller, M. L. (1912), The New Madrid earthquakes, *U.S. Geol. Surv. Bull.*, *494*, 119 pp.

Gan, W., and W. H. Prescott (2001), Crustal deformation rates in central and eastern U.S. inferred from GPS, *Geophys. Res. Lett.*, *28*, 3733–3736, doi:10.1029/2001GL013266.

Grollimund, B., and M. D. Zoback (2001), Did deglaciation trigger intraplate seismicity in the New Madrid Seismic Zone?, *Geology*, *29*, 175–178, doi:10.1130/0091-7613(2001)029<0175:DDTISI>2.0.CO;2.

Gutenberg, B., and C. F. Richter (1944), Frequency of earthquakes in California, *Bull. Seismol. Soc. Am.*, *34*, 185–188.

Hough, S. E. (2001), Triggered earthquakes and the 1811–1812 New Madrid, central U.S. earthquake sequence, *Bull. Seismol. Soc. Am.*, *91*, 1574–1581, doi:10.1785/0120000259.

Hough, S. E. (2009), Cataloging the 1811–1812 New Madrid, central U.S. earthquake sequence, *Seismol. Res. Lett.*, *80*, 1045–1053, doi:10.1785/gssrl.80.6.1045.

Hough, S. E., and S. Martin (2002), Magnitude estimates of two large aftershocks of the 16 December, 1811 New Madrid earthquake, *Bull. Seismol. Soc. Am.*, *92*, 3259–3268, doi:10.1785/0120010226.

Hough, S. E., and P. Pande (2007), Quantifying the "media bias" in intensity surveys: Lessons from the 2001 Bhuj, India earthquake, *Bull. Seismol. Soc. Am.*, *97*, 638–645, doi:10.1785/0120060072.

Hough, S. E., J. G. Armbruster, L. Seeber, and J. F. Hough (2000), On the modified Mercalli intensities and magnitudes of the 1811–1812 New Madrid, central United States earthquakes, *J. Geophys. Res.*, *105*, 23,839–23,864, doi:10.1029/2000JB900110.

Hough, S. E., R. Bilham, K. Mueller, W. Stephenson, R. Williams, and J. Odum (2005), Wagon loads of sand blows in White County, Illinois, *Seismol. Res. Lett.*, *76*, 373–386, doi:10.1785/gssrl.76.3.373.

Johnston, A. C. (1996a), Seismic moment assessment of earthquakes in stable continental regions I. Instrumental seismicity, *Geophys. J. Int.*, *124*, 381–414, doi:10.1111/j.1365-246X.1996.tb07028.x.

Johnston, A. C. (1996b), Seismic moment assessment of earthquakes in stable continental regions III, New Madrid 1811–1812, Charleston 1886, and Lisbon 1755, *Geophys. J. Int.*, *126*, 314–344, doi:10.1111/j.1365-246X.1996.tb05294.x.

Johnston, A. C., and E. S. Schweig (1996), The enigma of the New Madrid earthquakes of 1811–1812, *Annu. Rev. Earth Planet. Sci.*, *24*, 339–384, doi:10.1146/annurev.earth.24.1.339.

Kenner, S. J., and P. Segall (2000), A mechanical model for intraplate earthquakes: Application to the New Madrid Seismic Zone, *Science*, *289*, 2329–2332, doi:10.1126/science.289.5488.2329.

Liu, L. B., M. D. Zoback, and P. Segall (1992), Rapid interplate strain accumulation in the New Madrid Seismic Zone, *Science*, *257*, 1666–1669, doi:10.1126/science.257.5077.1666.

Mazzotti, S., T. S. James, J. Henton, and J. Adams (2005), GPS crustal strain, postglacial rebound, and seismic hazard in eastern North America: The Saint Lawrence valley example, *J. Geophys. Res.*, *110*, B11301, doi:10.1029/2004JB003590.

Mitchell, L., M. Magnani, K. McIntosh, B. Waldron, S. Saustrup, and M. Towle (2008), Recent deformation in the Mississippi embayment from high-resolution reflection data, *Eos Trans. AGU, 89*, Fall Meet. Suppl., Abstract S43A-1873.

Mitchill, S. L. (1815), A detailed narrative of the earthquakes which occurred on the 16th day of December, 1811, *Trans. Lit. Philos. Soc. N. Y.*, *1*, 281–307.

Mueller, K., and J. Pujol (2001), Three-dimensional geometry of the Reelfoot blind thrust: Implications for moment release and earthquake magnitude in the New Madrid Seismic Zone, *Bull. Seismol. Soc. Am.*, *91*, 1563–1573, doi:10.1785/0120000276.

Mueller, K., S. E. Hough, and R. Bilham (2004), Analysing the 1811–1812 New Madrid earthquakes with recent instrumentally recorded aftershocks, *Nature*, *429*, 284–288, doi:10.1038/nature02557.

Newman, A., S. Stein, J. Weber, J. Engeln, A. Mao, and T. Dixon (1999), Slow deformation and lower seismic hazard at the New Madrid Seismic Zone, *Science*, *284*, 619–621, doi:10.1126/science.284.5414.619.

Nuttli, O. W. (1973), The Mississippi Valley earthquakes of 1811 and 1812: Intensities, ground motion, and magnitudes, *Bull. Seismol. Soc. Am.*, *63*, 227–248.

Nuttli, O. W. (1979), Seismicity of the central United States, *Rev. Eng. Geol.*, *IV*, 67–93.

Obermeier, S. F. (1989), The New Madrid earthquakes: An engineering-geologic interpretation of relic liquefaction features, *U.S. Geol. Surv. Prof. Pap.*, *1336-B*, 114 pp.

Obermeier, S. F. (1996), Use of liquefaction-induced features for paleoseismic analysis: An overview of how seismic liquefaction features can be distinguished from other features and how their regional distribution and properties of source sediment can be used to infer the location and strength of Holocene paleo-earthquakes, *Eng. Geol.*, *44*, 1–76, doi:10.1016/S0013-7952(96)00040-3.

Obermeier, S. F., J. R. Martin, A. D. Frankel, T. L. Youd, P. J. Munson, C. A. Munson, and E. C. Pond (1993), Liquefaction evidence for one or more strong Holocene earthquakes in the Wabash Valley of southern Indiana and Illinois, with a preliminary estimate of magnitude, *U.S. Geol. Surv. Prof. Pap.*, *1536*, 26 pp.

Odum, J. K., W. J. Stephenson, K. M. Shedlock, and T. L. Pratt (1998), Near-surface structural model for deformation associated with the February 7, 1812, New Madrid, Missouri, earthquake, *Geol. Soc. Am. Bull.*, *110*, 149–162, doi:10.1130/0016-7606(1998)110<0149:NSSMFD>2.3.CO;2.

Page, M., K. Felzer, R. Weldon, and G. Biasi (2008), The magnitude-frequency distribution on the southern San Andreas fault follows the Gutenberg-Richter distribution, *Eos Trans. AGU*, *89*(53), Fall Meet. Suppl., Abstract S31C-06.

Penick, J. L., Jr. (1981), *The New Madrid Earthquakes*, rev. ed., Univ. of Mo. Press, Columbia.

Petersen, M. D., et al. (2008), Documentation for the 2008 update of the United States national seismic hazard maps, *U.S. Geol. Surv. Open File Rep.*, *OF 08–1128*.

Seeber, L., and J. G. Armbruster (1991), NCEER-91 earthquake catalog: Improved intensity-based magnitudes and recurrence relations for U.S. earthquakes, *NCEER-91–0021*, 110 pp., Natl. Cent. for Earthquake Eng. Res., Buffalo, N. Y.

Stein, S., and M. Liu (2009), Long aftershock sequences within continents and implications for earthquake hazard assessment, *Nature*, *462*, 87–89, doi:10.1038/nature08502.

Street, R. (1982), A contribution to the documentation of the 1811–1812 Mississippi Valley earthquake sequence, *Earthquake Notes*, *53*, 39–52.

Street, R. (1984), The historical seismicity of the central United States: 1811–1928: Final report, contract 14–08–0001–21251, Append. A, 316 pp., U.S. Geol. Surv., Washington, D. C.

Szeliga, W., S. E. Hough, S. Martin, and R. Bilham (2010), Intensity, magnitude, location, and attenuation in India for felt earthquakes since 1762, *Bull. Seismol. Soc. Am.*, *100*, 570–584, doi:10.1785/0120080329.

Tuttle, M. P., and E. S. Schweig (1996), Recognizing and dating prehistoric liquefaction features: Lessons learned in the New Madrid Seismic Zone, central United States, *J. Geophys. Res.*, *101*, 6171–6178, doi:10.1029/95JB02894.

Tuttle, M. P., E. S. Schweig, J. D. Sims, R. H. Lafferty, L. W. Wolf, and M. L. Haynes (2002), The earthquake potential of the New Madrid Seismic Zone, *Bull. Seismol. Soc. Am.*, *92*, 2080–2089, doi:10.1785/0120010227.

Tuttle, M. P., E. S. Schweig, J. Campbell, P. M. Thomas, J. D. Sims, and R. H. Lafferty (2005), Evidence for New Madrid earthquakes in A.D. 300 and 2350 B.C., *Seismol. Res. Lett.*, *76*, 489–501, doi:10.1785/gssrl.76.4.489.

Wald, D. J., V. Quitoriano, T. H. Heaton, and H. Kanamori (1999), Relationships between peak ground acceleration, peak ground velocity, and modified Mercalli intensity in California, *Earthquake Spectra*, *15*, 557–564, doi:10.1193/1.1586058.

Wells, D. L., and K. J. Coppersmith (1994), New empirical relationships among magnitude, rupture length, rupture width, rupture area, and surface displacement, *Bull. Seismol. Soc. Am.*, *84*, 974–1002.

Wessel, P., and W. H. F. Smith (1999), Free software helps map and display data, *Eos Trans. AGU*, *72*(41), 441.

Wu, P., and P. Johnston (2000), Can deglaciation trigger earthquakes in North America?, *Geophys. Res. Lett.*, *27*, 1323–1326, doi:10.1029/1999GL011070.

S. E. Hough and M. Page, U.S. Geological Survey, 525 South Wilson Ave., Pasadena, CA 91106, USA. (hough@usgs.gov)